Time-domain high-finesse atom interferometry

H. Hinderthür, F. Ruschewitz, H.-J. Lohe, S. Lechte, K. Sengstock, and W. Ertmer
Institut für Quantenoptik der Universität Hannover, Welfengarten 1, D-30167 Hannover, Germany
(Received 13 March 1998; revised manuscript received 30 June 1998)

We report on experiments of multiple-beam atom interferometry in the time domain. Laser-cooled and trapped atoms interact with atomic ''multiple beam splitters'' realized by time sequences of resonant laser pulses. The output signals of the interferometers show Fabry-Perot-like high-finesse interference structures. The number of interfering de Broglie waves is adjustable and in principle not limited in this scheme. We present the experimental realization of up to 160 interfering partial waves. [S1050-2947(99)04303-6]

PACS number(s): 03.75.Dg, 39.20.+q, 39.30.+w, 42.50.−p

The field of atom optics has undergone a tremendous development in recent years. Various atom-optical devices have been demonstrated, e.g., lenses, mirrors, beam splitters, and diffraction gratings [1]. Interferometers for atoms have proven to have excellent properties for measurements in fundamental and applied research [2].

As is well known from light optics, multiple-beam interferometry has the potential for strong improvements of the achievable sensitivities. In addition, interference of multiple beams is the key principle for atom resonators as they are currently being discussed. The experimental preparation of atomic high-finesse interferometry with a large number of partial beams has not been studied so far.

Very recently, first atomic multiple-beam interferometers have been demonstrated [3,4]. In those experiments the number of interfering waves was limited to a finite number of internal atomic substates which are involved in the coherent beam-splitting process. Therefore those concepts in principle cannot be extended to high-finesse interferometers [5].

In this paper we report on the realization of a scheme for atomic multiple-beam interferometry where, in contrast to previous experiments, the interference process occurs in the time domain. In the context of interferometric precision measurements, time domain interferometry [6–10] with laser-cooled and trapped atoms is most promising regarding the possibility of long interaction times. Our multiple-beam atom interferometer concept combines the advantages of time domain interferometry with the important aspect that an internal two-level scheme is sufficient for the multiple-beam preparation. Moreover, the number of interfering atomic partial waves in the interferometer is variable within a wide range. Therefore, our concept allows systematic studies of high-finesse atomic interferences.

In Fig. 1 the principle of time domain atom interferometry with multiple beams is shown in a space-time representation. An atomic ''multiple beam splitter'' is realized by a time sequence of N laser pulses of frequency ω_L interacting with cold atoms nearly at rest. The interaction is resonant with an internal atomic two-level system (of eigenfrequency ω_0) with an excited state lifetime long enough to neglect spontaneous processes. Thus each interaction coherently splits the atomic wave into two partial waves associated with different center of mass momenta. Accordingly, the atomic paths separate in space. Interference between different atomic partial waves requires spatial overlap between the corresponding paths. This spatial overlap between up to N different atomic waves is provided by the application of a second sequence of N counterpropagating laser pulses. Moreover, an N-beam interferometer is characterized by the interference of N different waves with phase differences $n\Phi_0$ ($n=1,\ldots,N-1$), where Φ_0 gives the phase difference between two neighboring waves. In our interferometer, atomic partial waves in the excited state accumulate phases $e^{-i\omega_0 T}$ due to their quantum-mechanical state evolution during the dark times T (Fig. 1). The different paths spend different times in the excited state. Additional phases $e^{\mp i\omega_L t_i}$ are transferred as a consequence of the absorption and emission of laser photons at interaction times t_i ($i=1,\ldots,2N$). The summed-up phase differences $\delta\Phi_n$ between the N atomic partial waves at the interferometer exit in Fig. 1 then turn out to be

$$\delta\Phi_n = n\Phi_0 = n\Delta 2T \quad (n=1,\ldots,N-1), \tag{1}$$

where $\Delta=\omega_L-\omega_0$ denotes the laser detuning from resonance and T is the time period between two successive laser pulses of a sequence.

In conclusion, the geometry in Fig. 1 satisfies the two conditions for an N-beam interferometer mentioned above [11]. Note that the phases in Eq. (1) are similar to phases appearing in classical Ramsey spectroscopy [12]. As a result of the frequency-dependent phase differences, interference patterns appear as a function of the laser detuning Δ from resonance.

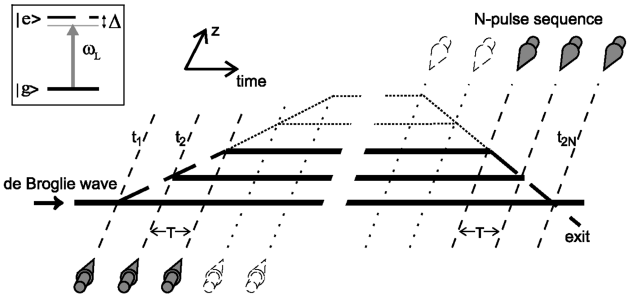

FIG. 1. Simplified sketch of the time domain atomic multiple-beam interferometer (bold lines indicate the special case of $N=3$; dotted arrows indicate optionally added laser pulses). Each laser pulse sequence represents a variable ''multiple beam splitter'' for atomic de Broglie waves. Inset, internal atomic two-level transition.

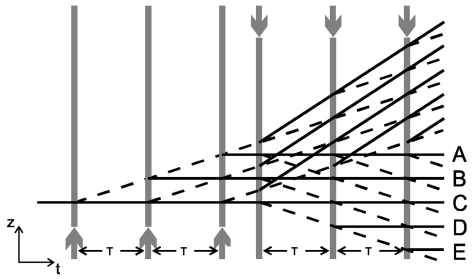

FIG. 2. All possible paths for an interferometer with three-pulse laser sequences (gray, laser pulse sequences; black, all possible atomic trajectories; solid lines, ground state; dashed lines, excited state; *A* to *E*, ground-state exit ports of one group of trajectories).

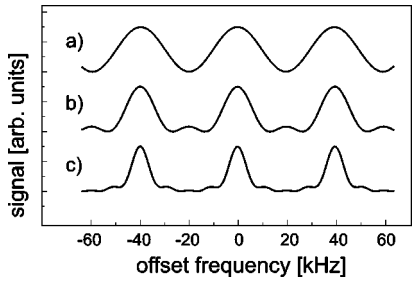

FIG. 3. Calculated interference signals for the ground-state exits. All amplitudes are normalized: (a) two-pulse, (b) three-pulse, and (c) five-pulse excitation.

Whereas Fig. 1 is showing only the essential atomic paths, $2N$ successive laser interactions prepare in general a splitting into 2^{2N} atomic trajectories. These trajectories lead to different spatially separated exit ports which show interferences of different orders. A sketch of all possible paths for an interferometer with three-pulse sequences is shown in Fig. 2.

The interesting and important feature of our scheme is that the highest order interference clearly dominates the overall signal. Below we will give a brief discussion on the individual signal contributions to illustrate this aspect for the case of three-pulse excitation.

In Fig. 2 the first beam-splitter sequence (first three pulses) prepares $2^3=8$ trajectories leading to six different paths in the central dark zone. Among these six paths, three correspond to atomic waves in the ground state and three to waves in the excited state. In the following sequence, these two sets develop into two so-called recoil components, each consisting of 32 different trajectories. The interference processes within each of the two recoil components are equivalent, resulting in two sets of interference fringes split by twice the photon recoil $\delta(\delta=\hbar k^2/2M$, where k and M denote the laser wave vector and the atomic mass). The following discussion is limited to the high-frequency recoil component featuring ground-state trajectories in the central dark zone.

The corresponding five ground-state exits in Fig. 2 are denoted by *A* to *E*. Typically the spatial separation (along the *z* axis) between the exits is small compared to the extension of the atomic ensemble. According to this, interferences are read out state-selectively. As a consequence, the signals are a superposition of the contributions from all exits belonging to the same internal state.

The exits *A* and *E* are reached by one trajectory each. Thus the signals from *A* and *E* show no interference pattern and produce a frequency-independent constant background. The signals from exits *B* and *D* show identical pure two-beam interferences. In exit *C* six trajectories are recombined. Among these, four are in-phase and form a three-beam interference with the other two waves. Generally in a three-beam interferometer the interference signal *S* is characterized by two different oscillatory terms and can be expressed as

$$S=A_1\cos(\delta\Phi_1)+A_2\cos(\delta\Phi_2),\quad \delta\Phi_2=2\,\delta\Phi_1, \qquad (2)$$

where in the case of our three-pulse interferometer $\delta\Phi_1$ and $\delta\Phi_2$ are given by Eq. (1). For an ''ideal'' three-beam interference the ratio $A_1{:}A_2$ is 2:1 [13]. Analytical calculations for our three-pulse interferometer give this ratio as 16:9 for a chosen optical pulse area of $\Omega_{\mathrm{Rabi}}\tau=\pi/3$. Thus the overall output signal of the scheme in Fig. 2 is close to the signal of an ''ideal'' three-beam interferometer. Analogous calculations show that the application of two counterpropagating *N*-pulse sequences in general prepare *N*-beam interferences. This will be published elsewhere.

In Fig. 3, calculated signals for two-, three-, and five-pulse sequences are shown. The calculations in Fig. 3 use numerical solutions of the optical Bloch equations analogous to the case of two-pulse laser interactions ($N=2$) [14] and include the photon recoil and all experimental parameters. For a photon recoil of $\delta=39.8$ kHz, a chosen periodicity of 39.8 kHz ensures constructive overlap between the interference signals of the two recoil components. Calculations and experimental data indicate that the signal contrast reaches a maximum for optical pulse areas of $\Omega_{\mathrm{Rabi}}\tau\approx\pi/N$. The signals in Fig. 3 clearly show the multiple-beam character of the interferometer concept and verify that interferences of the highest order are predominating.

In the experiment, the atomic ensemble is formed by a magneto-optical trap (MOT) which is loaded from an effusive magnesium (^{24}Mg) atomic beam. The trap is operated by a frequency-doubled dye laser system tuned to the strong $^1S_0-{}^1P_1$ transition in Mg at 285 nm. The temperature of the trapped atoms is close to the Doppler limit at 1.9 mK. Under typical experimental conditions we store up to 10^5 atoms. For the beam-splitting transition we use the $^1S_0-{}^3P_1$ intercombination line at 457 nm with an upper state natural lifetime of 5.1 ms. The 457 nm light is supplied from a frequency-stabilized dye laser spectrometer with a laser linewidth of below 1 kHz [15].

Each interferometry cycle is started by switching off the MOT. Then the two *N*-pulse beam-splitter sequences are applied to the freely expanding cloud of atoms. Each cycle is completed by switching on the trap again. A photomultiplier records the fluorescence signal which is a direct measure of the trap population. Atoms which remain in the metastable excited state after an interferometry cycle are not recaptured when the trap is switched on. Thus the ground-state interference signals are encoded in the remaining trap fluorescence after recapturing. Details of the detection scheme are given in [7]. We switch between interferometry and trapping with a rate of typically 50 Hz.

Figure 4 shows typical experimental results. From top to

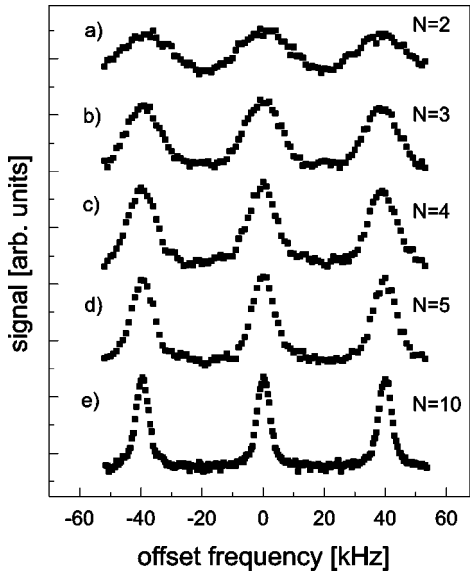

FIG. 4. Atomic multiple-beam interferometer signals for different numbers of interfering beams. From (a) to (e), the corresponding optical pulse widths are 6 μs, 4 μs, 3 μs, 2.4 μs, and 1.2 μs. The integration time per data point is 5 s. The left axis scale is identical for all plots.

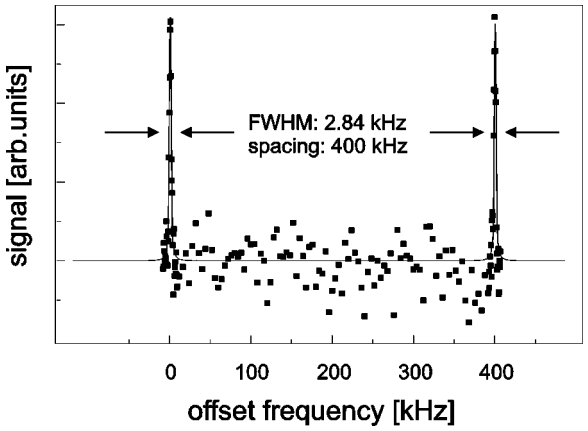

FIG. 5. Atomic high-finesse interferences for 160 interfering beams (finesse $F=140.8$). The pulse width is 75 ns. The integration time per datum is 14.4 s. For comparison, the amplitude of the calculated signal (solid line) was fitted to the data maxima.

bottom the graphs correspond to interferences of two, three, four, five, and ten partial de Broglie waves. As in Fig. 3, we chose a periodicity of 39.8 kHz. This corresponds to a time period of about 12.6 μs between two successive laser pulses in each sequence. According to a Rabi frequency of about $\Omega_{\mathrm{Rabi}}=2.6\times10^{5}\ \mathrm{s}^{-1}$, a pulse width of $\tau=12$ μs represents an optical π pulse. So the pulse widths corresponding to the data in Fig. 4 have been adjusted to 6 μs, 4 μs, 3 μs, 2.4 μs, and 1.2 μs (corresponding to π/N pulses). The shape of the experimental signals is in good agreement with our calculations. Figure 4(a) shows a purely sinusoidal structure well known from two-beam interferometry. For the three-pulse excitation [Fig. 4(b)], a significant deviation from the sinusoidal shape is obvious. The full width at half maximum (FWHM) of the main maxima is 12.9 ± 0.4 kHz, which corresponds to a reduction in fringe width by about 36%. This narrowing effect is stronger than the one observed in [4]. The four- and five-beam interference signals [Fig. 4(c) and Fig. 4(d)] show further systematic narrowing. Down to the ten-beam interference signals in Fig. 4(e), the fringe amplitudes do not decrease. Note that the width of the fringes in Fig. 4 is determined by the effective measurement time $2(N-1)T$, which is increased from (a) to (e). Each interference signal is Heisenberg-limited.

Due to the fact that the spectral width of the excitation profile is broadened for shorter pulses, a larger velocity class of atoms in the MOT takes part in the interference process as the number of partial beams is increased. This additional effect is most obvious for the transition from two- to three-beam interference where the fringe amplitude is strongly enhanced by about 60%.

Figure 5 shows interference signals for 160 pulses per sequence corresponding to up to 160 partial atomic waves interfering with each other. The dark time period between successive pulses is 1.25 μs, resulting in a periodicity of 400 kHz. In this measurement the interference signal of the high-frequency recoil component is suppressed by destroying the coherence of all ground-state trajectories in the central dark zone. This is done by additional photon scattering on the fast trapping transition at 285 nm (see also Ref. [16]). The solid line represents a numerical calculation for the low-frequency component of the signal. The peaks in Fig. 5 show a FWHM of 2.84 ± 0.20 kHz. The ratio between spacing and FWHM is 140.8. To our knowledge, this represents the highest atom-optical finesse which has been observed so far.

At present the contrast of the high-finesse signals is limited by the finite time resolution of our pulse generator producing distorted pulse shapes for pulse widths below 100 ns. In principle, our interferometer concept allows the realization of atomic interferences with even higher finesse. Compared to the previously demonstrated atomic multiple-beam interferometers, our time domain concept has the main advantage of an adjustable number of interfering de Broglie waves and independence from the actual atomic level scheme. Note that this concept also offers new possibilities for other types of atom interferometers, e.g., the Ramsey Bordé interferometer with Raman transitions [6].

In conclusion we have presented a multiple-beam atom interferometer, the signals of which are comparable to those of an optical Fabry-Pérot interferometer. Our concept opens up the possibility to observe atomic interferences with considerably high finesse. In contrast to optical Fabry-Pérot interferometers in this time domain experiment with atoms nearly at rest, no spatial transmission pattern appears. A detailed discussion of analogies and differences will be given in a forthcoming presentation. Due to its model character, our interferometer represents a tool for systematic investigation of atomic multiple-beam interferences. Experiments concerning the decoherence properties of this kind of atom interferometer under the influence of single photon scattering are in progress.

The authors appreciate many contributions to the experimental setup by J. L. Peng and proofreading by J. Burghardt. This work has been supported by the Deutsche Forschungsgemeinschaft under Grant No. SFB 407.

[1] See, e.g., C. S. Adams, M. Sigel, and J. Mlynek, Phys. Rep. **240**, 143 (1994).

[2] See, e.g., *Atom Interferometry*, edited by P. Berman (Academic Press, San Diego, 1997).

[3] M. Weitz, T. Heupel, and T. W. Hänsch, Phys. Rev. Lett. **77**, 2356 (1996).

[4] H. Hinderthür, A. Pautz, V. Rieger, F. Ruschewitz, J. L. Peng, K. Sengstock, and W. Ertmer, Phys. Rev. A **56**, 2085 (1997).

[5] In atom interferometers which are working with microfabricated gratings, the beam-splitting process is also based on interference of multiple atomic beams. For detailed description, see the articles by J. Schmiedmayer *et al.*, J. F. Clauser and S. Li, and B. Dubetsky and P. R. Berman in Ref. [2].

[6] M. Kasevich and S. Chu, Phys. Rev. Lett. **67**, 181 (1991).

[7] K. Sengstock, U. Sterr, G. Hennig, D. Bettermann, J. H. Müller, and W. Ertmer, Opt. Commun. **103**, 73 (1993).

[8] Th. Kisters, K. Zeiske, F. Riehle, and J. Helmcke, Appl. Phys. B: Lasers Opt. **59**, 89 (1994).

[9] P. Szriftgiser, D. Guéry-Odelin, M. Arndt, and J. Dalibard, Phys. Rev. Lett. **77**, 4 (1996).

[10] S. B. Cahn, A. Kumarakrishnan, U. Shim, T. Sleator, P. R. Berman, and B. Dubetsky, Phys. Rev. Lett. **79**, 784 (1997).

[11] Setups for multiple laser interactions with atomic beams have been realized in A. G. Adam, T. E. Gough, N. R. Isenor, G. Scoles, and J. Shelley, Phys. Rev. A **34**, 4803 (1986) and A. Morinaga, *ibid.* **45**, 8019 (1992). As these experiments feature space-domain interferometers, the interaction times and interference periodicities are feathered out due to a wide range of atomic velocities.

[12] N. F. Ramsey, Phys. Rev. **78**, 695 (1950).

[13] B. Vittoz, Helv. Phys. Acta **26**, 400 (1953).

[14] C. J. Bordé, C. Salomon, S. Avrillier, A. van Lerberghe, C. Bréant, D. Bassi, and G. Scoles, Phys. Rev. A **30**, 1836 (1984).

[15] F. Ruschewitz, J. L. Peng, H. Hinderthür, N. Schaffrath, K. Sengstock, and W. Ertmer, Phys. Rev. Lett. **80**, 3173 (1998).

[16] F. Riehle, J. Ishikawa, and J. Helmcke, Phys. Rev. Lett. **61**, 2092 (1988).